Bioremediation Journal, 12(2):98–110, 2008

ISSN: 1088-9868
DOI: 10.1080/10889860802060469

Taylor & Francis
Taylor & Francis Group

Increased Capacity for Polycyclic Aromatic Hydrocarbon Mineralization in Bioirrigated Coastal Marine Sediments

Michael T. Montgomery,[1]
Christopher L. Osburn,[1]
Yoko Furukawa,[2]
and Joris M. Gieskes[3]
[1]Naval Research Laboratory, Code 6114, Washington, DC, USA
[2]Naval Research Laboratory, Code 7431, Stennis Space Center, Mississippi, USA
[3]Marine Research Division, Scripps Institution of Oceanography, University of California at San Diego, La Jolla, California, USA

ABSTRACT Bioirrigation of marine sediments by benthic infauna has the potential to increase both the rate and depth of bacterial mineralization of polycyclic aromatic hydrocarbons (PAHs) by recirculating oxygenated bottom water into sediment burrows. Rates of heterotrophic bacterial production and mineralization of PAHs (naphthalene, phenanthrene, and fluoranthene) were measured in sections of sediment cores sampled from stations in San Diego Bay. Data suggest that rates of PAH biodegradation and bacterial heterotrophy were influenced by bioirrigation by benthic infauna. PAH mineralization and heterotrophic production were higher in core sections where sulfide was not detected relative to core sections containing sulfide. Depth-integrated capacity of the upper 17 cm of sediment to mineralize PAHs was 4 to 10 times higher at the station with bioirrigation coefficients that increased with depth. Remedial dredging of sediments to remove contaminant mass (and presumable lower ecological risk) will also remove benthic infauna. Removal of infauna and the subsequent lowering of bioirrigation in surface sediments would be expected to lower the capacity of intrinsic PAH bioremediation. This could cause local increases in ambient PAH concentration and consequently increase the ecological risk at the site and potentially degrade the health of the ecosystem by removing a sink for PAHs.

KEYWORDS bacterial production, bioirrigation, intrinsic, marine, mineralization, PAH, radiotracers, sediment

Disclosure. The opinions and assertions contained herein are not to be construed as official or reflecting the views of the U.S. Navy or the Federal Government at large. Mention of trade names or commercial products does not constitute endorsement or recommendation for use.

Address correspondence to Michael T. Montgomery Naval Research Laboratory, Code 6114, 4555 Overlook Avenue, Washington, DC 20375, USA. E-mail: michael.montgomery@nrl.navy.mil

INTRODUCTION

Polycyclic aromatic hydrocarbon (PAH)-degrading bacteria are ubiquitous in estuarine and marine sediments and are commonly found in areas that do not have substantial known PAH sources (Chung and King, 2001). Rapid PAH catabolism generally depends on molecular oxygen availability to sedimentary bacteria (Cerniglia, 1992; Chung and King, 1999; Leahy and Olsen, 1997), though recently, PAH mineralization has been coupled with other redox processes, such as sulfate reduction (Coates et al., 1998; Hayes and Lovely, 2002; Zhang and Young, 1997; Bedessem et al., 1997) and nitrification (Deni and

Penninckx, 1999; Bonin et al., 1994; Gilewicz et al., 1991). In unperturbed, organic carbon–enriched sediment, heterotrophic bacterial metabolism rapidly depletes oxygen, limiting its availability to the top few millimeters of sediment (Rasmussen and Jorgensen, 1992). Processes that mix the sediment with oxygenated bottom waters can increase the amount of oxygen available to bacteria that are deeper in the sediment. One of these processes involves the activities of benthic infauna that excavate and mix large portions of the sediment and then ventilate their burrows (Aller, 1988).

Bioirrigation has been linked to dramatic changes in both the composition and metabolic activity of the sedimentary bacterial assemblage (see review by Kogure and Wada, 2005; Cuny et al., 2007). Macrofaunal burrows harbor unique assemblages of bacteria that mineralize PAHs more rapidly than those from adjacent, nonburrowed sediment (Chung and King, 1999, 2001; Holmer et al., 1997; Madsen et al., 1997; Schaffner et al., 1997; Bauer et al., 1988; Granberg et al., 2005). Madsen et al. (1997) found that the depth-integrated removal of fluoranthene was twice as high when capitellids worms were present. Bauer et al. (1988) had similar findings with regards to anthracene degradation by capitellids. The activity of diverse macrofaunal communities has also been linked to seasonal removal of PAHs and polychlorinated biphenyls (Schaffner et al., 1997). These findings have led several researchers to postulate that the relative abundance and composition of benthic macroorganism communities control the rate of bacterial PAH degradation in marine sediment (Madsen et al., 1997). Chung and King (2001) concluded that the capacity for PAH biodegradation in hydrocarbon-impacted ecosystems depends on the composition of the natural bacterial assemblage and its response to environmental parameters, rather than on the introduction of new taxa (bioaugmentation). The activities of the benthic macrofauna may create an environment that preferentially selects PAH-degrading bacteria and these activities may increase the depth of the transition zones within the sediment that are important to enhancing bacterial metabolism (Bauer et al., 1988; Ghiorse et al., 1995; Polerecky et al., 2006).

Dredging, a commonly considered remedial alternative for reducing the ecological risk of PAH-impacted submerged sediments, is thought to be beneficial to the health of the ecosystem. However, in addition to the PAHs, benthic infauna are also removed and their pore water mixing activities (i.e., bioirrigation) are likewise disrupted. If bioirrigation enhances intrinsic PAH biodegradation by sedimentary bacteria, then the physical removal of infauna may negatively affect the capacity of the ecosystem to biologically remove PAHs from the watershed. Though there has been much work on the impact of PAH on macrofaunal communities (see review by Fleeger et al., 2003; Carman et al., 1995, 1996), there are few studies providing a quantitative measure of intrinsic PAH bioremediation capacity in coastal sediments. To study the latter, rates of heterotrophic bacterial production and mineralization of naphthalene, phenanthrene, and fluoranthene were measured in sections of sediment cores sampled from two stations in an urbanized waterway in San Diego Bay, CA. The microbial studies were accompanied by pore water chemical studies to establish the redox conditions of the sediments. Pore water chemistry was described by chemical analysis of pore water extracted by centrifugation. The combination of sediment chemistry, modeling, and microbial ecology techniques were used to examine the effects of bioirrigation on the capacity of the natural microbial assemblage to naturally attenuate PAHs.

MATERIAL AND METHODS

Site Description and Sampling

Paleta Creek is an urbanized waterway that receives surface runoff from the adjacent Naval Station and downtown San Diego. Station P17 (longitude: 117.1160° W; latitude: 32.6738° N; water depth: ~6 m) is near the headwaters of the creek and station P04 (longitude 117.1211°W; latitude: 32.6715° N; water depth: ~11 m) is closer to the confluence with San Diego Bay (Figure 1). Sediment at the study site was primarily fine grained (major mode $\geq 4\Phi$) (Germano, 2002), with organic carbon content ranging from 1.1% to 1.7% at station P04 and 1.1% to 2.9% at station P17.

In January 2002, four adjacent cores were taken from each station using a multicore sampler and transferred intact to the laboratory and at ambient temperature within 3 h of collection. Two 5-cm diameter cores from each station were sectioned (2 to 3 cm each) and subsampled for PAH concentration, bacterial production, and mineralization of PAH (e.g., naphthalene, phenanthrene, and fluoranthene). Two other adjacent cores were sectioned for measurement of pore water composition. Slurries for biological assays were made from filtered water overlying the respective cores.

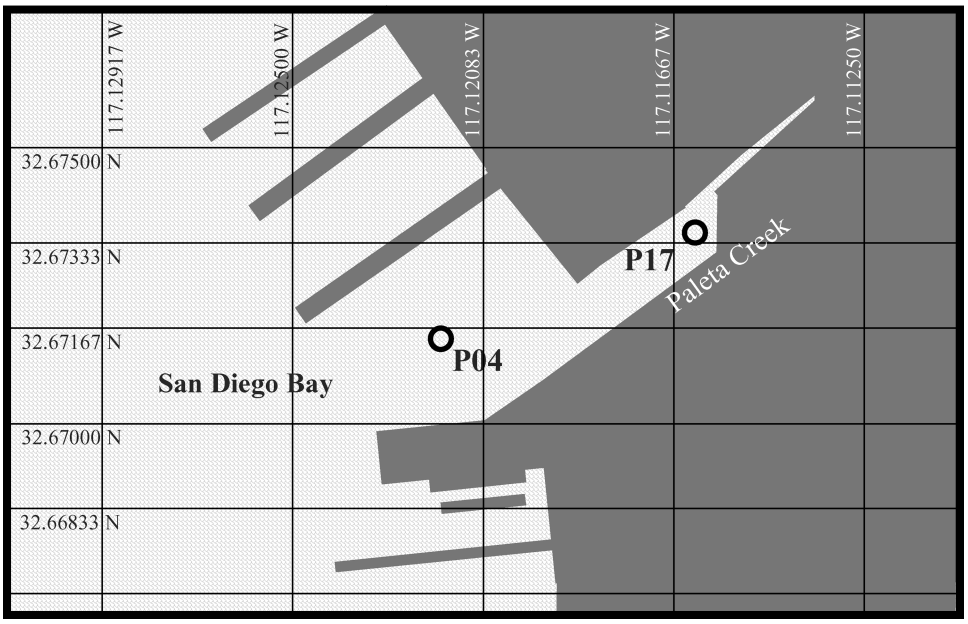

FIGURE 1 **Sampling locations for stations P17 and P04 in Paleta Creek in San Diego Bay, CA.**

Heterotrophic Bacterial Production

The leucine incorporation method (Kirchman et al., 1985; Kirchman, 1993; Smith and Azam, 1992) was used to measure bacterial production as adapted by Montgomery et al. (1999). A 50-μl sample of wet sediment from each core section was added to 2-ml microcentrifuge tubes sealed with screw caps with O-rings (Fisher Scientific; three experimental and one killed control), which were precharged with [^{3}H-4,5]-l-leucine (20 nM final concentration; specific activity: 154 mCi mmol^{-1}; Sigma). The sediment was extracted from the core section and added to the microfuge tube using a 1-cm^3 plastic syringe with the end cut off. One milliliter of filtered (0.45-μm nominal pore diameter; Acrodisk, Gelman) bottom water (collected from above the upper core section) was then added to each tube to form a sediment slurry. Samples were incubated for 2 h at in situ temperatures and subsequently processed by the method of Smith and Azam (1992). Incubations were ended by adding 57 μl of 100% trichloroacetic acid (TCA; 5% final concentration; Fisher Scientific). Killed controls had the TCA added prior to the addition of the sediment and their values were subtracted from those of the experimental samples. A constant isotope dilution factor of two was used for all samples. This was estimated from actual measurements of sediment dissolved free amino acids (Burdige and Martens, 1990) and saturation experiment estimates (Tuominen, 1995). Samples of wet sediment at 1 cm^3 were dried at 50°C to a constant mass to convert production values to dry weight. Leucine incorporation rate was converted to bacterial carbon using factors determined by Simon and Azam (1989) and the formula of Smith and Azam (1992).

Pore Water Chemistry

Pore water samples were obtained by centrifugation (Sorval; 10,000 $\times$ *g*) under nitrogen to prevent oxidation of labile components (e.g., Fe^{2+} and HS^-). Iron was determined by inductively coupled plasma–optical emission spectra (ICP-OES). Alkalinity was determined by acidimetric titration, whereas ammonium, sulfide, sulfate, and phosphate were determined by spectrophotometry (Gieskes et al., 1991).

PAH Degradation

Mineralization Rates

PAH mineralization assays were initiated within 3 h of sediment sample collection using a modification of Boyd et al. (2005) and Pohlman et al. (2002). Three sentinel PAHs (Sigma) were used as radiotracers: uL-^{14}C-naphthalene (specific activity: 18.6 mCi mmol^{-1}), 3-^{14}C-fluoranthene (45 mCi mmol^{-1}), and 9-^{14}C-phenanthrene (55.7 mCi mmol^{-1}). They were added in separate incubations (triplicate live samples and one killed control) to sediment samples (1 cm^3 wet volume) from each core section in 100 $\times$16-mm

polystyrene test tubes to a final concentration of about 0.2 μg g^{-1} (depending on specific activity). Isotope dilution was calculated from the ambient PAH concentration in an attempt to keep additions to less than 10% of ambient concentrations so that it is a radiotracer of assemblage degradation rate and not a calculation of biodegradation potential (see also Deming, 1993). Samples were incubated for 24 h at in situ temperature to minimize bacterial assemblage change, and evolved $^{14}CO_2$ was captured on NaOH-soaked filter papers. H_2SO_4 (2 ml, 2 N) was added to end incubations, kill the control, and partition remaining CO_2 into headspace of the tube and ultimately to the filter paper trap. The filter paper traps containing metabolized $^{14}CO_2$ were removed, radioassayed and then used to calculate substrate mineralization.

PAH Concentration

Ambient PAH concentrations of 18 semivolatile United States Environmental Protection Agency (US EPA) priority pollutants were determined using the US EPA SW 8270 method (Fisher et al., 1997). Briefly, 10 to 15 g of sediment was dried with diatomaceous earth and then extracted in methanol and methylene chloride using standard accelerated solvent extraction. The extracts were concentrated under a N_2 stream (Speedvap) and analyzed by GC/MS (Fisher et al., 1997). *p*-Terphenyl-d_{14} and 2-fluorobiphenyl were used as surrogate standards, with modifications described in Pohlman et al. (2002).

Turnover Time

The turnover time was calculated by dividing the ambient concentration of phenanthrene or fluoranthene (μg kg^{-1}; naphthalene was below detection limits of 1.00 $\times$ 10^{-3} μg kg^{-1} day^{-1}) with the mineralization rate (μg kg^{-1} day^{-1}). This value (in days) is a measure of the average residence time of an individual PAH molecule in the ambient pool of PAH in the sediment. Rapid turnover times (days to weeks) are characteristic of transient compounds that are rapidly metabolized by the natural heterotrophic bacteria assemblage. Slow turnover times (years to decades) suggest that there are relatively low rates of intrinsic bioremediation of these compounds as molecules entering the pool have a long residence time within the sediment.

Capacity for Intrinsic Biodegradation

The intrinsic degradation capacity of a sediment column was calculated by multiplying the mineralization rate of 1 wet cm^3 (the actual unit of measure of the assay) by the depth of the core that was sampled (17 cm). The mineralization values for 0 to 1 cm and 1 to 2 cm were taken from the 0 to 2 cm mineralization measurement, whereas the values for 8 to 9, 9 to 10, and 10 to 11 cm were taken from the 8 to 11 cm mineralization value. These average values for each cm^3 were then summed for a sediment column of 1 cm $\times$ 1 cm $\times$ 17 cm for each of the three cores, giving a degradation capacity of each core. This capacity was then extrapolated to 1 m $\times$ 1 m $\times$ 17 cm (multiply by 10,000) to put the analyses in units that would be useful in management of contaminated sediments or an ecosystem level evaluation.

Modeling Approach

An inverse modeling approach (Berg et al., 1998; Meile et al., 2001; Furukawa et al., 2004) was used to quantify biological pore water mixing (i.e., bioirrigation) and consequential deep O_2 fluxes at stations P04 and P17. MatLab software (Mathworks, Natick, MA) was used for all numerical modeling.

Determination of α through Inverse Modeling

The objective of inverse modeling was to determine the irrigation coefficient, α, as a function of depth (x). The inverse model used in this study was based on the one-dimensional (1D) mass conservation equation for solute species in which molecular diffusion, bioirrigation, and production/consumption reactions were considered to dominate chemical mass transport:

$$\frac{\partial C}{\partial t} = D' \frac{\partial^2 C}{\partial x^2} + \alpha(C_0 - C) + \Sigma R \qquad (1)$$

(Berner, 1980), in which the time- (t) dependent concentration of a dissolved species (C) along the vertical axis (x) was determined by its diffusive transport (with D' being the tortuosity-corrected molecular diffusion coefficient (Boudreau, 1996)), transport by bioirrigation (with α being the bioirrigation coefficient [Emerson et al., 1984]), and net rate of production and consumption reactions (ΣR). The use of Equation (1) assumes chemical mass transfer due to sediment accumulation,

erosion, and compaction to be negligible (Boudreau, 1996).

The partial discretization of Equation (1) for the i-th node on a vertical grid yields:

$$\frac{dC_i}{dt} = D'_i \frac{C_{i+1} - 2C_i + C_{i-1}}{\Delta x^2} + \alpha_i (C_0 - C_i) + \Sigma R_i \quad (2)$$

(Boudreau, 1996). C_i and D'_i denote the concentration and diffusion coefficient at the i-th node, respectively, and Δx is the distance between adjacent nodes.

By assuming that the geochemical profiles were at steady state, the left-hand side of Equation (2) was set to zero, and the right-hand side was reorganized as:

$$aa_i C_{i-1} + bb_i C_i + cc_i C_{i+1} + dd_i = 0 \quad (3)$$

where

$$aa_i = \frac{D'}{(\Delta x)^2} \quad (4\text{-}1)$$

$$bb_i = -\frac{2D'}{(\Delta x)^2} - \alpha_i \quad (4\text{-}2)$$

$$cc_i = \frac{D'}{(\Delta x)^2} \quad (4\text{-}3)$$

$$dd_i = \alpha_i C_0 + \Sigma R_i \quad (4\text{-}4)$$

It should be noted that the assumption of steady state means that there was a balance between the flux (due to accumulation or loss to the water column), intrasediment transport (due to molecular diffusion and bioirrigation), and reaction (either production or consumption). If known concentrations are used at WSI (i.e., $x = 0$, 1st node), C_0, and at the bottom of the modeled sediment column (i.e., $x = L_b$, n-th node), C_b, as the boundary condition, the following equations can also be written:

$$C_{i=1} = C_0 \quad (5\text{-}1)$$

$$C_{i=n} = C_b \quad (5\text{-}2)$$

Consequently, the series of equations can be written as:

$$\begin{pmatrix} bb_1 & cc_1 & & & & & \\ aa_2 & bb_2 & cc_2 & & & & \\ & aa_3 & bb_3 & cc_3 & & & \\ & & \ddots & & & & \\ & & & \ddots & & & \\ & & & aa_i & bb_i & cc_i & \\ & & & & \ddots & & \\ & & & & & \ddots & \\ & & & & aa_{n-1} & bb_{n-1} & cc_{n-1} \\ & & & & & aa_n & bb_n \end{pmatrix} \begin{pmatrix} C_1 \\ C_2 \\ C_3 \\ \vdots \\ C_{i-1} \\ C_i \\ C_{i+1} \\ \vdots \\ C_{n-1} \\ C_n \end{pmatrix} + \begin{pmatrix} dd_1 \\ dd_2 \\ dd_3 \\ \vdots \\ dd_{i-1} \\ dd_i \\ dd_{i+1} \\ \vdots \\ dd_{n-1} \\ dd_n \end{pmatrix} = 0 \quad (6\text{-}1)$$

or

$$ABC \cdot C + DD = 0 \quad (6\text{-}2)$$

in which C and DD are vectors and ABC is a tridiagonal matrix.

Inverse Modeling Strategy for Rate Determination

Equations (2) through (6) show that α is the only unknown if depth dependent values of C and ΣR are known a priori. Depth-concentration profiles of dissolved inorganic carbon (DIC; as approximated by alkalinity) were available from P17 and P04, and the net production rate of DIC was estimated from the leucine incorporation rate, assuming a linear correlation between bacterial production and carbon metabolism with a 30 % growth efficiency to calculate CO_2 evolution (Benner et al., 1988). Thus, the modeling proceeds by: (1) calculating the concentration profiles (C_{calc}) for DIC by initially using randomly assigned values for the α profile; and (2) iteratively refining the α profile by seeking to minimize the difference between calculated (C_{calc}) and measured or interpolated ($C_{measured}$) profiles for DIC.

A simple matrix manipulation of equation (6-2) yields:

$$C = -ABC^{-1} \cdot DD \quad (7)$$

Consequently, the calculated concentration of DIC at i-th node can be expressed as a function of *a priori* parameters as well as α using:

$$C_{calc,i} = F_1(D', \alpha_i, \Sigma R_i) \quad (8)$$

In practice, the inverse determination of the α profile progresses as follows. First, a randomly generated set of initial values are assigned to $\alpha_1, \alpha_2, \ldots, \alpha_i, \ldots \alpha_n$. It is assumed that α remains constant within each 0.005 m vertical section. Then, using the set of α values in Equation (7), a DIC concentration profile is calculated (i.e., $C'_{calc,1} C'_{calc,2} \cdots, C'_{calc,i} \cdots, C_{calc,n}$). Next, the differences between measured/interpolated and calculated concentration profiles is evaluated as follows:

$$\Sigma F = \sum_{i=1}^{n} \frac{|C_{calc,i} - C_{measured,i}|}{C_{measured,i}} \qquad (9)$$

Subsequently, α_i values are iteratively adjusted to find the optimized set of values until the value of ΣF is minimized according to the trust region methods for nonlinear minimization (Coleman and Li, 1996). The routine used is that supplied in the Matlab Optimization Toolbox. To ensure that the optimization process leads to the global minima rather than the local minima, the process is repeated up to 50 times, each with a new, randomly generated initial α values (Meile et al., 2001).

Forward Calculation of Depth-Concentration Profiles

Once the depth profile of α was determined through inverse modeling, it was used in the forward modeling to confirm that the calculated depth profiles DIC were in agreement with measured profiles. In the forward modeling, Equation (2), an ordinary differential equation (ODE) after the partial discretization, was written for DIC, and solved for C_i's by integrating dC/dt over time using the stiff ODE solver built in Matlab (ode23tb). The series of Equation (2) was written for each node and parameterized using the same D' and ΣR values used in the inverse modeling above.

RESULTS AND DISCUSSION

Heterotrophic Bacterial Production

Heterotrophic bacterial production (as measured by the leucine incorporation method) represents a standard measure of growth and carbon metabolism in aquatic systems. Rates are generally much higher in mixed aerobic systems than in static, anaerobic environments. In San Diego Bay, bacterial production was highest near the sediment-water interface, ranging from 297 to 11.9 μg C kg^{-1} day^{-1} with depth at P04 and from 198 to 6.00 μg C kg^{-1} day^{-1} with depth at P17 (Figure 2). Production was highest in the uppermost (0 to 2 cm below surface) section in all three core profiles.

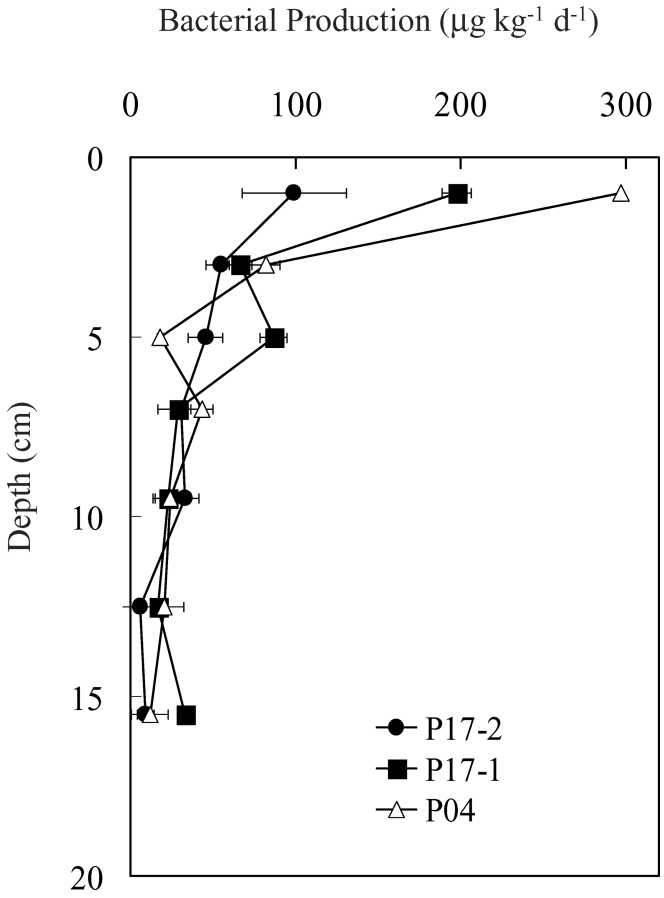

FIGURE 2 **Bacterial production (μg C kg^{-1} day^{-1}) with depth (cm) for cores from stations P17 and P04. Error bars on bacterial production are the standard deviation of triplicate samples.**

Pore Water Chemistry

With depth in the sediment from the sediment-water interface, manganese and iron oxides are often generated between the zones of dissolved oxygen (DO) and sulfate reduction. Based on chemical analyses of the pore water from San Diego cores, sulfide was not detected in the P04 cores using spectrophotometry but increased with depth in the P17 cores (Figure 3A), whereas sulfate decreased in concentration (Figure 3B). Alkalinity in the P04 cores showed little change with depth from the sediment-water interface, whereas there is an increase with depth in the P17 cores (Figure 3C). Manganese oxide reduction at station P17 occurs immediately at or below the sediment water interface, followed by a rapid decrease within the upper 1 to 2 cm

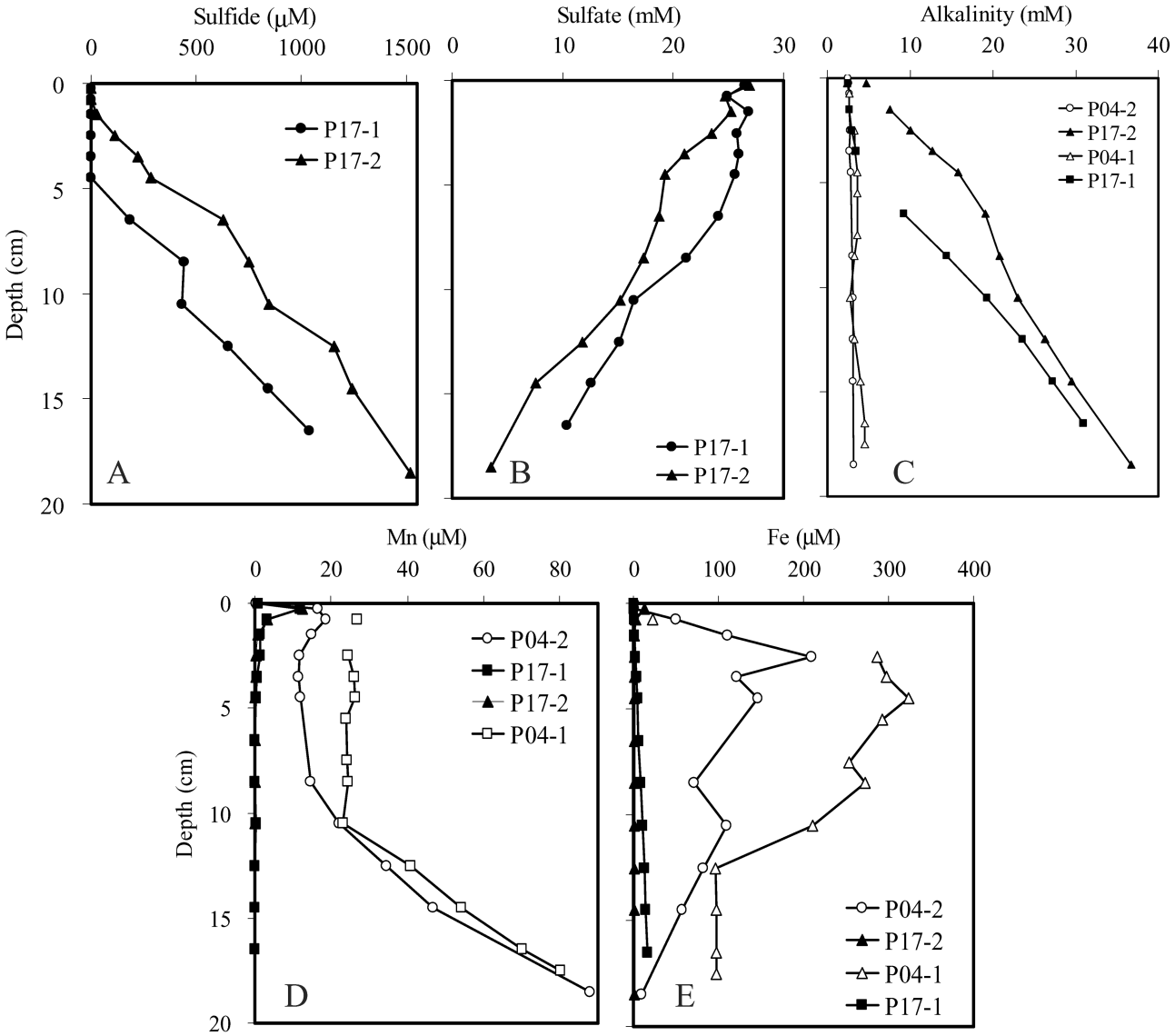

FIGURE 3 **Pore water concentrations for sulfide (A), sulfate (B), alkalinity (C), manganese (D), and iron (E) for P17 (filled) and P04 (empty) cores.**

(Figure 3D). Similarly, dissolved iron maxima occur at or very near the core surface, followed by a rapid decrease, partially controlled by iron sulfide solubility (Figure 3E). At station P04, dissolved manganese rapidly increases near the surface sediment, followed by a secondary increase below ~10 cm (Figure 3D), i.e., in the zone of initial sulfate reduction. These profiles suggest that the pore water from the P04 cores is more frequently mixed with bottom water at the sediment-water interface than is the pore water from P17.

PAH Mineralization and Turnover

Total PAH concentration in the P17 cores ranged from 1.19 to 3.18 μg g^{-1} (8 to 11 cm section), whereas PAH concentration at P04 ranged from 0.40 to 1.16 μg g^{-1} (14 to 17 cm section; Figure 4). Ambient naphthalene concentrations were below detection (0.01 ppm) in all core sections for the two stations, so turnover time could not be calculated. Naphthalene mineralization rates were also low with most sections below the detection level (1.00×10^{-3} μg kg^{-1} day^{-1}) ranging up to 2.65 ($\pm$0.19) μg kg^{-1} day^{-1} (average of replicate measurements $\pm 1\ \sigma$), but most values were not differentiable from the killed control (Table 1). Although naphthalene flux through the sediments cannot be determined based on ambient concentration, given the transient nature of this compound and the low mineralization rates, there does not appear to be rapid intrinsic bioremediation of this PAH in these

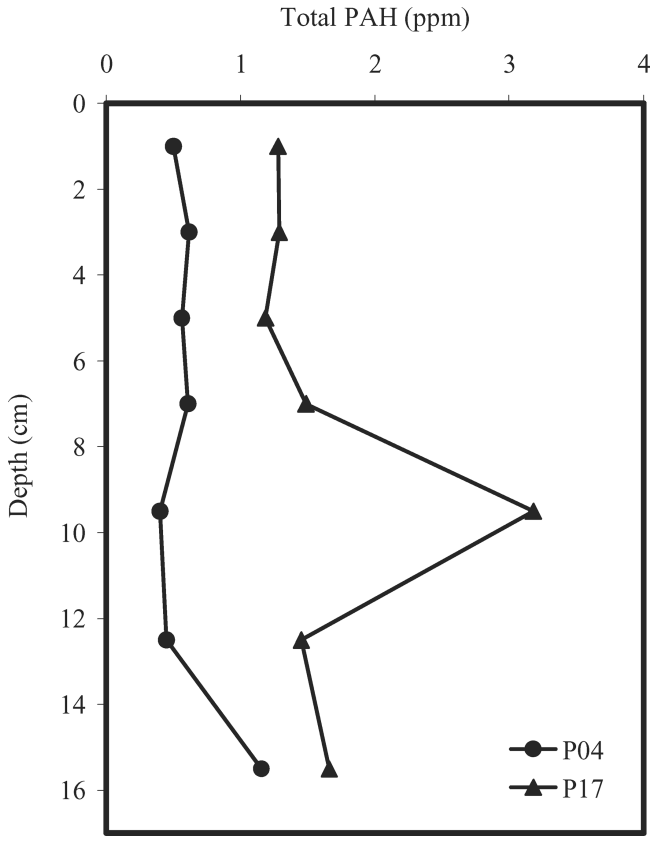

FIGURE 4 **Total PAH concentrations (ppm) with depth (cm) for core sections from P17 for P04 cores.**

sediments. This is expected given that the low ambient concentrations and the assumed low flux of naphthalene would not provide selective pressure for naphthalene degrading bacteria amongst the natural microbial assemblage.

The ambient phenanthrene concentrations were higher than those for naphthalene, ranging from 0.03 to 0.06 μg g^{-1}at P17 and 0.02 to 0.03 μg g^{-1}at P04, and mineralization rates were also higher ranging from below detection to 3.48 ($\pm$1.2) μg kg^{-1} day^{-1} at P17 and 2.69 ($\pm$0.73) to 8.57 ($\pm$5.5) μg kg^{-1} day^{-1} at P04. These phenanthrene mineralization rates are similar to those found for core slices in Eagle Harbor, WA sediments using longer incubation times (ca. 2 μg kg^{-1} day^{-1} calculated from Tang et al., 2006). Phenanthrene turnover time was similar between the two P17 cores, ranging from 14 to 119 days with P17-1 and 28 to 77 days with P17-2. Turnover time was much more rapid throughout the entire 17 cm at P04, ranging from 3 to 8 days. This suggests that the natural bacterial assemblage was rapidly processing phenanthrene molecules that were migrating into the top cm of sediment at P04. Biological mixing of the deeper sediments with bottom water particles or nepheloid layer material depositing onto the surface sediments from the water column could comprise such a flux of PAH to depth (Baker et al., 1991).

The ambient fluoranthene concentration in the sediments ranged from 0.09 to 0.38 μg g^{-1} at P17 and 0.05 to 0.10 μg g^{-1} at P04, whereas mineralization rates ranged from below detect to 1.09 ($\pm$0.54) μg kg^{-1} day^{-1} at P17 and 0.18 ($\pm$0.18) to 5.09 ($\pm$0.81) μg kg^{-1} day^{-1} at P04 (Table 1). Fluoranthene turnover time with the two P17 cores ranged from 236 to 1598 days with P17-1 and 193 to 1632 days with P17-2. The turnover time was much more rapid throughout the entire 17 cm at P04, ranging from 5 to 91 days. These PAH turnover times were within the seasonal range of 6 to 160 days (Pohlman et al., 2002) and 17 to 430 days (phenanthrene; Boyd et al., 2005) reported for surface sediments in the Delaware River estuary. Looking only at surface sediments (within 0.1 cm of the sediment-water interface), Boyd et al. (2005) found a relationship between fluoranthene mineralization rates and seasonal fluctuations in DO concentrations. The finding that elevated mineralization rates occur only when DO is above 70% saturation (Boyd et al., 2005) reinforces the connection between the biological mixing activities of benthic infauna and the rates of intrinsic hydrocarbon bioremediation by bacteria.

The presence of hydrogen sulfide in core sections would be indicative of marine sediments that were poorly bioirrigated or otherwise unmixed with the overlying aerobic water column. For each core, values for bacterial production and PAH mineralization were averaged for core sections where no sulfide was detected by spectroscopy (upper sections) and compared with those averaged among sections where sulfide was detected (deeper sediments). Bacterial production in upper sediments without sulfide was about three to five times the average of that in the lower sulfidic sediments (Table 2). Average PAH mineralization rates were always higher (up to ten times) in nonsulfidic sediment sections than in the poorly mixed sulfidic sediments (Table 2). This comparison of rates between the sulfidic and nonsulfidic regions within each core further supports a positive relationship between bioirrigation and PAH mineralization.

TABLE 1 **Average (AVG) and Standard Deviation (*SD*) of PAH Mineralization Rates and Turnover Time**

		Mineralization rate (μg C kg^{-1} day^{-1})							
		Naphthalene		Phenanthrene		Fluoranthene		Turnover time (days)	
Core	Depth (cm)	AVG	SD	AVG	SD	AVG	SD	Phenanthrene	Fluoranthene
P17-1	0–2	1.06	0.162	3.48	1.20	0.445	0.232	14	530
	2–4	0.271	0.0416	0.435	0.180	0.105	0.114	119	1598
	4–6	0	0	0.592	0.128	0.244	0.177	90	436
	6–8	0	0	0.990	0.812	0	0	59	ND
	8–11	0	0	1.42	0.700	1.09	0.543	35	345
	11–14	0	0	0.418	0.080	0	0	78	ND
	14–17	0	0	0.718	0.526	0.497	0.056	60	236
P17-2	0–2	0	0	1.20	1.05	0.848	0.275	42	278
	2–4	0.521	0.031	0.742	0.125	0	0	70	ND
	4–6	0.064	0.007	0	0	0.065	0.029	ND	1632
	6–8	1.05	0.126	0.758	0.392	0.615	0.291	77	250
	8–11	0	0	1.73	0.547	0.476	0.166	28	790
	11–14	0.049	0.002	1.37	0.484	0.608	0.215	31	193
	14–17	0.284	0.009	0.762	0.245	0.133	0.048	43	684
P04	0–2	0	0	7.86	1.07	5.09	0.807	3	20
	2–4	2.65	0.193	8.57	5.50	1.80	1.75	3	5
	4–6	0	0	3.53	0.508	2.38	1.85	7	27
	6–8	0	0	5.09	2.13	1.99	1.37	6	43
	8–11	0	0	2.69	0.726	0.790	0.491	8	67
	11–14	0.183	0.021	5.02	1.32	0.872	0.149	5	91
	14–17	0	0	3.51	0.602	3.07	2.52	4	15

Note. Mineralization rates and turnover time were measured for each of the three cores with depth (cm). ND = not determined.

Determination of Bioirrigation Coefficient, α

Net Rate (ΣR) of DIC Production as a Function of Depth

The net rate of DIC production was estimated from heterotrophic bacterial production measurements. Bacterial production rate profiles for P17-1, P17-2, and P04 were expressed in terms of the bacterial carbon produced (μg) per kg of dry sediments per day (Figure 2). With average sediment porosity of 60% and a dry sediment density (i.e., grain density) of 2.65, the bacterial carbon production rate can be expressed in terms of moles L^{-1} of pore water s^{-1} by multiplying by the factor of 1.70×10^{-12} (i.e., $= 10^{-6} \times \frac{1}{12} \times \frac{1}{\frac{1}{2.65} \times \frac{0.6}{1-0.6}} \times \frac{1}{24 \times 60 \times 60}$). The conversion is necessary because DIC is reported in terms of moles L^{-1}. Further, these values were converted to the rate of DIC production by using the bacterial growth efficiency of 30 % (Benner et al., 1988) by multiplying by 2.33 (i.e., = 0.7/0.3).

Other Parameters

The depth profiles of DIC concentrations, C_i's, were assumed to be equal to the measured alkalinity (i.e.,

TABLE 2 **Bacterial Production and PAH Mineralization Rate Averages**

		AVG rate of core section (μg C kg^{-1} day^{-1})	
Rate parameter	Station	No sulfide	Sulfide present
Bacterial production	P17	99.4	33.4
	P04	110.1	18.9
Naphthalene mineralization	P17	0.48	0.20
	P04	0.66	0.06
Phenanthrene mineralization	P17	0.68	0.33
	P04	2.53	1.54
Fluoranthene mineralization	P17	0.42	0.35
	P04	6.88	0.88

Note. Bacterial production and PAH mineralization rate averages were higher for core sections that did not have sulfide present compared with those that had measurable sulfide concentrations.

Figure C). The tortuosity-corrected diffusion coefficient, D', was estimated from the following relationship between porosity φ (= 0.6), bottom water temperature T (= 20°C), and infinite-dilution diffusion coefficient for bicarbonate ion HCO_3^-, $D^0_{HCO_3^-}$ (Boudreau, 1996):

$$D^0_{HCO_3^-} = (5.06 + 0.275 \times T) \times 10^{-6} \mathrm{cm^2 s^{-1}}$$

$$D' = \frac{D^0_{HCO_3^-}}{1 - \ln(\varphi^2)} = 5.22 \times 10^{-6} \mathrm{cm^2 s^{-1}}$$

Inversely Determined α

The depth profiles of α for cores P17-1, P17-2, and P04 were determined through inverse modeling (Figure 5). The model-derived irrigation coefficients indicated that (1) biological pore water mixing was focused within the upper ~4 cm of sediments at P17-1, whereas it intensified at a deeper portion of the sediments (~9 to 14 cm) at P04; and (2) biological pore water mixing was very heterogeneous since two cores from P17 exhibited very different α profiles (i.e., significant bioirrigation in P17-1 in the top 4 to 6 cm, and virtual lack of bioirrigation in P17-2). These high α values were similar to those reported from other heavily irrigated harbor sediments such as Buzzard Bay, Massachusetts (Martin and Banta, 1992) and New York Bay (Komada et al., 2004).

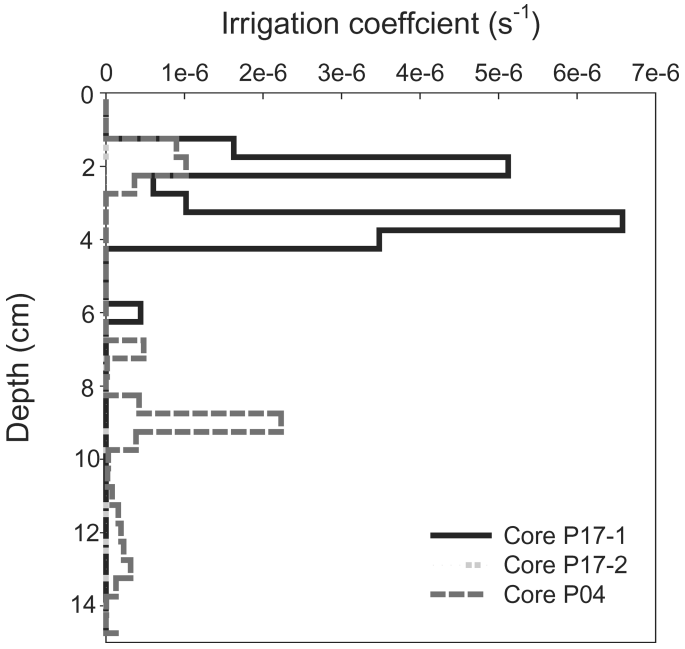

FIGURE 5 **Model-calculated irrigation coefficients are shown as functions of depth. The model results indicate that the DIC profile of core P17-1 was a result of strong bioirrigation near the sediment-water interface, and that of core P04 was a result of deep-penetrating bioirrigation as a significant bioirrigation was hindcasted for 13 to 14 cm below the interface. The DIC profile of core P17-2 indicates a lack of bioirrigation.**

There is a positive linear relationship between irrigation coefficients and the availability of an interface between the burrow wall and oxygenated burrow water (Koretsky et al., 2002). In turn, there is a positive correlation between the burrow wall surface area and diffusive oxygen flux (Wenzhöfer and Glud, 2004). Thus, the high α value in the deeper part of P04 directly indicates a high O_2 flux. Although irrigation coefficients are often thought to decrease with depth (Martin and Banta, 1992), subsurface maxima in profiles have been determined using a similar inverse model technique in Buzzards Bay and Washington Shelf (Meile et al., 2001). High PAH mineralization rates found in the deeper part of P04 corroborate the large values of α estimated for the deeper part of P04.

Intrinsic Biodegradation Capacity

Irrigation coefficients were greater than 10^{-7} cm^2 s^{-1} throughout the core at P04 but only in the top four cm of core P17-1 and in no section of core P17-2. The intrinsic biodegradation capacity for each station was determined based on the mineralization rates of each core section integrated to the 17 cm depth of each core. Though there was some difference in the modeled effect of bioirrigation in the top four cm between cores P17-1 and P17-2, there was little difference in calculated intrinsic biodegradation capacity for naphthalene (27 versus 43 μg C m^{-2} day^{-1}), phenanthrene (187 versus 170 μg C m^{-2} day^{-1}), and fluoranthene (64 versus 67 μg C m^{-2} day^{-1}) when integrated over the entire depth of the cores (Table 3). At station P04, the intrinsic PAH biodegradation capacity was slightly higher for naphthalene (58 μg C m^{-2} day^{-1}), and much higher for phenanthrene (837 μg C m^{-2} day^{-1}), and fluoranthene (692 μg C m^{-2} day^{-1}) (Table 3). Because most of the capacity for PAH mineralization of the station P17 cores was in the top several centimeters, making measurements on deeper cores would not be expected to substantially increase the calculated biodegradation capacity at the station. In the case of station P04, however, bioirrigation extended throughout the 17 cm depth of the core and may have occurred in deeper regions thus making this a conservative estimate of intrinsic PAH biodegradation capacity.

In site investigations of US coastal sediments, the ambient PAH concentration is typically considered

TABLE 3 **Irrigation Coefficient and Intrinsic Degradation Rates**

Core	Irrigation coefficient 10^{-7} cm^2 s^{-1} (depth, cm)	Intrinsic biodegradation capacity (μg C m^{-2} day^{-1} for top 17-cm sediment)		
		Naphthalene	Phenanthrene	Fluoranthene
P17-1	0–4	27	187	64
P17-2	0	43	170	67
P04	0–17	58	837	692

Note. The irrigation coefficient was greater than 10^{-7} cm^2 s^{-1} in the top 0 to 4 cm at P17 but extended throughout the 17-cm depth of the core from P04. The intrinsic degradation rates for each PAH were used to calculate the degradation capacity of 1 m^2 of surface sediment integrated to the 17-cm depth of the core measurements.

to be the result of historical anthropogenic inputs as EPA guidance focuses on comparison with historical land use of areas adjacent to the site rather than on tracking contaminant flux to the sediment (e.g. via sediment traps; http://www.epa.gov/waterscience/cs/). However, the sediment-water interface in coastal ecosystems is frequently impacted by dynamic processes involving tides, rain events, ship traffic and bioturbation. As PAH concentrations increase in the sediment, so does the selective pressure for PAH degrading bacteria amongst the natural microbial assemblage (Roch and Alexander, 1997; Aelion et al., 1989). In dynamic environments, the ambient PAH concentration is more likely the result of a balance between PAH flux to the surface sediments (sedimentation of PAHs on particles) and removal processes (biodegradation, chemical transformation).

In a related study, Chadwick et al. (2006) estimated rates of particle-bound PAH flux to the sediment at stations P04 and P17 using data collected from sediment traps deployed during the two weeks prior to this study. They found that particle-associated deposition of naphthalene, phenanthrene and fluoranthene was 0.47, 31.2, and 54.0 μg m^2 day^{-1} (respectively) at station P17, and 0.74, 17.1, and 32.1 μg m^2 day^{-1} (respectively) at station P04 (Chadwick et al., 2006). Total PAH concentration in the sediment trap material ranged from 9.7 to 41.6 μg g^{-1} (Chadwick et al., 2006), which is much higher than that found in the underlying sediment (0.4 to 3.18 μg g^{-1}; Figure 5). This analysis does not include episodic PAH inputs from oil spills or rain events, nor are there measures of PAH flux to or from the station via lateral transport in the bottom boundary layer. Notwithstanding these potential errors, the intrinsic biodegradation capacity of the mixed surface sediments at station P04 exceeds the PAH flux due to sedimentation. The flux of naphthalene, phenanthrene and fluoranthene to the surface sediment at P04 is matched by the bacterial mineralization of those compounds in a column of sediment less than 1 cm deep (0.03, 0.54, and 0.63 cm, respectively). At P17, naphthalene and phenanthrene flux would be matched by the mineralization rate in a column of sediment 0.09 and 2.41 cm deep, respectively. However it would take a mixed sediment layer of 12.2 cm deep to match the fluoranthene flux, thus fluoranthene could be accumulating at station P17.

CONCLUSIONS

In the US federal and state regulatory community overseeing the management of contaminated sediment, there is a widespread belief that mass removal always lowers ecological risk at an impacted site. It is also widely held that PAH biodegradation only occurs in the top several mm of sediment due to rapid depletion of oxygen in marine sediments. However, the mixing activities of benthic infauna can dramatically change the composition of electron acceptors deep within sediment through reoxygenation. Within a sediment core, sections that did not contain sulfide exhibited higher rates of PAH mineralization than those that contained sulfide, even in core sections that were 17 cm below the sediment-water interface. Because sulfide is rapidly oxidized in the presence of oxygen, it was clear that the higher rates of PAH mineralization were due to the presence of oxygen, which can be attributed to bioirrigation. In addition, the more bioirrigated sediment station (based on biogeochemistry and modeling of irrigation coefficients) had a higher capacity for intrinsic biodegradation of phenanthrene and fluoranthene. Remedial dredging activities may have the unintended effect of disrupting the relationship between PAH degrading bacteria and benthic infauna, inadvertently reducing the

intrinsic PAH bioremediation capacity of the ecosystem.

This work adds to the published literature demonstrating the association between the activity of benthic infauna and PAH degradation by natural bacterial assemblages in coastal sediments. More importantly, this represents the first attempt to provide a quantitative measure of intrinsic PAH biodegradation in submerged coastal sediments. The type of evaluation used here can give site managers and regulators a decision-making tool for evaluating ecological risk reduction due to intrinsic bioremediation relative to engineering solutions, such as remedial dredging.

ACKNOWLEDGEMENTS

This work was supported by SERDP (CU-1209) for "Pathway interdiction: a system for evaluating and ranking sediment contaminant pathways in support of in-place management" to S. Apitz & B. Chadwick (M.T.M., C.L.O., and J.M.G.) and the Office of Naval Research (to M.T.M. and C.L.O.) Contract No. N0001499WX20525. The authors thank V. Kirtay, B. Chadwick, E. Arias, and J. Groves for assistance in sampling and J. Germano for technical assistance and discussions, as well as for the comments and corrections of two anonymous reviewers. The authors thank A. DeLozier for formatting the manuscript.

REFERENCES

Aelion, C. M., D. C. Dobbins, and F. K. Pfaender. 1989. Adaptation of aquifer microbial communities to the biodegradation of xenobiotic compounds: Influence of substrate concentration and preexposure. *Environ. Toxicol. Chem. 8*:75–86.

Aller, R.C. 1988. Benthic fauna and biogeochemical processes in marine sediments: The role of burrow structures. In:*Nitrogen cycling in coastal marine environments*, ed. T. H. Blackburn and J. Sorensen, 301–338. Chichester, England: Wiley.

Baker, J. E., S. J. Elsenreich, and B. J. Eadie. 1991. Sediment trap fluxes and benthic recycling of organic carbon, polycyclic aromatic hydrocarbon, and polychlorobiphenyl congeners in Lake Superior. *Environ. Sci. Technol. 25*:500–509.

Bauer, J. E., R. P. Kerr, M. F. Bautista, C. J. Decker, and D. G. Capone. 1988. Stimulation of microbial activities and polycyclic aromatic hydrocarbon degradation in marine sediments inhabited by *Capitella capitata. Mar. Environ. Res. 25*:63–84.

Bedessem, M. E., N.G. Swoboda-Colberg, and P.J. S. Colberg. 1997. Naphthalene mineralization coupled to sulfate reduction in aquifer-derived enrichments. *FEMS Microbiol. Lett. 152*:213–218.

Benner, R., J. Lay, E. K'Nees, and R. E. Hodson. 1988. Carbon conversion efficiency for bacterial growth on lignocellulose: implications for detritus-based Food Webs. *Limnol. Oceanogr. 33*:1514–1526.

Berg, P., N. Risgaard-Petersen, and S. Rysgaard. 1998. Interpretation of measured concentration profiles in sediment pore water. *Limnol. Oceanogr. 43*:1500–1510.

Berner, R.A. 1980. *Early Diagenesis; A Theoretical Approach*, 241. Princeton, NJ: Princeton University Press.

Bonin, P., E. R. Ranaivoson, N. Raymond, A. Chalamet, and J. C. Bertrand. 1994. Evidence for denitrification in marine sediment highly contaminated by petroleum products. *Mar. Poll. Bull. 28*:89–95.

Boudreau, B.P. 1996. *Diagenetic Models And Their Implementation: Modeling Transport And Reaction In Aquatic Sediments*, 414. New York: Springer-Verlag.

Boyd, T. J., M. T. Montgomery, J. K. Steele, J. W. Pohlman, S. R. Reatherford, B. J. Spargo, and D. C. Smith. 2005. Dissolved oxygen saturation controls PAH biodegradation in freshwater estuary sediments. *Microb. Ecol. 49*:226–235.

Burdige, D. J., and C. S. Martens. 1990. Biogeochemical cycling in an organic-rich marine basin—11: The sedimentary cycling of dissolved free amino acids. *Geochim. Cosmochim. Acta 54*:3033–3052.

Carman, K. R., J. W. Fleeger, J. C. Means, S. M. Pomarico, and D. J. McMillan. 1995. Experimental investigation of the effects of polynuclear aromatic hydrocarbons on an estuarine sediment food web. *Mar. Environ. Res. 40*:289–318.

Carman, K. R., J. C. Means, and S. C. Pomarico. 1996. Response of sedimentary bacteria in a Louisiana salt marsh to contamination by diesel fuel. *Aquat. Microb. Ecol. 10*:231–241.

Cerniglia, C.E. 1992. Biodegradation of polycyclic aromatic hydrocarbons. *Biodegrad. 3*:351–368.

Chadwick, D. B., V. Kirtay, A. C. Blake, E. Arias, B. Davidson, J. Guerrero, S. E. Apitz, J Germano., J. Maa, C. Smith, R. Paulsen, M. T. Montgomery, W. Ziebis, J. Gieskes, and J. Groves. 2006. Pathway Ranking for In-place Sediment Management (CU1209): Final Site II Report—Pearl Harbor. CU1209, Strategic Environmental Research and Development Program, 1–857. http://docs.serdp-estcp.org

Chung, W. K., and G. M. King. 1999. Biogeochemical transformations and potential polyaromatic hydrocarbon degradation in macrofaunal burrow sediments. *Aquat. Microb. Ecol. 19*:285–295.

Chung, W. K., and G. M. King. 2001. Isolation, characterization, and polyaromatic hydrocarbon degradation potential of aerobic bacteria from marine macrofaunal burrow sediments and description of *Lutibacterium anuloederans* gen. nov., sp. nov., and *Cycloclasticus spirillensus* sp. nov. *Appl. Environ. Microbiol. 67*:5585–5592.

Coates, J. D., D. J. Ellis, E.L. Blunt-Harris, C. V. Gaw, E. E. Roden, and D. R. Lovley. 1998. Recovery of humic-reducing bacteria from a diversity of environments. *Appl. Environ. Microb. 64*:1504–1509.

Coleman, T. F., and Y. Y. Li. 1996. An interior trust region approach for nonlinear minimization subject to bounds. *SIAM J. Optimiz. 6*:418–445.

Cuny, P., G. Miralles, V. Cornet-Barthaux, M. Acquaviva, G. Stora, V. Grossi, and F. Gilbert. 2007. Influence of bioturbation by the polychaete *Nereis diversicolor* on the structure of bacterial communities in oil contaminated coastal sediments. *Mar. Poll. Bull. 54*:452–459.

Deming, J.W. 1993. ^{14}C-tracer method for measuring microbial activity in deep sea sediments. In: *Handbook of Methods in Aquatic Microbial Ecology,* ed. P. F. Kemp, B. F. Sherr, E. B. Sherr, and J. J. Cole, 405–414. Boca Raton, FL: Lewis Publishers.

Deni, J., and M. J. Penninckx. 1999. Nitrification and autotrophic nitrifying bacteria in a hydrocarbon-polluted soil. *Appl. Environ. Microbiol. 65*:4008–4013.

Emerson, S., R. Jahnke, and D. Heggie. 1984. Sediment-water exchange in shallow-water estuarine sediments. *J. Mar. Res. 42*:709–730.

Fisher, J. A., M. J. Scarlett, and A. D. Stott. 1997. Accelerated solvent extraction: An evaluation for screening of soils for selected U.S. EPA semivolatile organic priority pollutants. *Environ. Sci. Technol. 31*:1120–1127.

Fleeger, J. W., K. C. Carman, and R. M. Nisbet. 2003. Indirect effects of contaminants in aquatic ecosystems. *Sci. Total Environ. 317*:207–233.

Furukawa, Y., A. C. Smith, J. E. Kostka, J. Watkins, and C. R. Alexander. 2004. Quantification of macrobenthic effects on diagenesis using a multicomponent inverse model in salt marsh sediments. *Limnol. Oceanogr. 49*:2058–2072.

Germano, J. 2002. Sediment profile Investigation of San Diego Harbor: An investigation of bioturbation depths for the pathway ranking for in-place sediment management (PRISM) project. In: *SERDP CU-1209 Pathway Ranking For In-Place Sediment Management (PRISM),* ed. B. Chadwick and S. E. Apitz, 23–64. Arlington, VA: Annual report to the Strategic Environmental Research and Development Program. http://docs.serdp-estcp.org

Ghiorse, W. C., J. B. Herrick, R. L. Sandoli, and E. L. Madsen. 1995. Natural selection of PAH-degrading bacterial guilds at coal-tar disposal sites. *Environ. Health Perspect*. 103:103–111.

Gieskes, J. M., T. Gamo, and H. Brumsack. 1991. Chemical methods for interstitial water analysis aboard JOIDES resolution. *Ocean Drilling Prog. Tech. Note* 15:60.

Gilewicz, M., G. Monpert, M. Acquaviva, G. Mille, and J.-C. Betrand. 1991. Anaerobic oxidation of 1-n-Heptradecene by a marine denitrifying bacterium. *Appl. Microbiol. Biotechnol. 36*:252–256.

Granberg, M. E., R. Hansen, and H. Selck. 2005. Relative importance of macrofaunal burrows for the microbial mineralization of pyrene in marine sediments: Impact of macrofaunal species and organic matter quality. *Mar. Environ. Prog. Ser. 288*:59–74.

Hayes, L. A., and D. R. Lovley. 2002. Specific 16S rDNA sequences associated with naphthalene degradation under sulfate-reducing conditions in harbor sediments. *Microb. Ecol. 43*:134–145.

Holmer, M., V. E. Forbes, and T. L. Forbes. 1997. Impact of the polychaete *Capitella* sp. 1 on microbial activity in an organic-rich marine sediment contaminated with the polycyclic aromatic hydrocarbon fluoranthene. *Mar. Biol. 128*:679–688.

Kirchman, D.L. 1993. Leucine incorporation as a measure of biomass production by heterotrophic bacteria. In: *Handbook of Methods In Aquatic Microbial Ecology,* ed. P. F. Kemp, B. F. Sherr, E. B. Sherr, and J. J. Cole, 509–512. Boca Raton, FL: Lewis Publishers.

Kirchman, D. L., E. K'Nees, and R. Hodson. 1985. Leucine incorporation and its potential as a measure of protein synthesis by bacteria in natural aquatic systems. *Appl. Environ. Microbiol. 49*:599–607.

Kogure, K., and M. Wada. 2005. Impacts of macrobenthic bioturbation in marine sediment on bacterial metabolic activity. *Microb. Environ. 20*:191–199.

Komada, T., C. E. Reimers, G. W. Luther, and D. J. Burdige. 2004. Factors affecting dissolved organic matter dynamics in mixed-redox to anoxic coastal sediments. *Geochem. Cosmichem. Acta 68*:4099–4111.

Koretsky, C. M., C. Meile, and P. Van Cappellen. 2002. Quantifying bioirrigation using ecological parameters: A stochastic approach. *Geochem. Trans. 3*:17–30.

Leahy, J. G., and R. H. Olsen. 1997. Kinetics of toluene degradation by toluene-oxidizing bacteria as a function of oxygen concentration, and the effect of nitrate. *FEMS Microbiol. Ecol. 23*:23–30.

Madsen, S. D., T. L. Forbes, and V. E. Forbes. 1997. Particle mixing by the polychaete *Capitella* species 1: Coupling fate and effect of a particle-bound organic contaminant (fluoranthene) in a marine sediment. *Mar. Ecol. Prog. Ser. 147*:129–142.

Martin, W. R., and G. T. Banta. 1992. The measurement of sediment irrigation rates—a comparison of the Br- tracer and Rn-222/Ra-226 disequilibrium techniques. *J. Mar. Res. 50*:125–154.

Meile, C., C. M. Koretsky, and P. Van Cappellen. 2001. Quantifying bioirrigation in aquatic sediments: an inverse modeling approach. *Limnol. Oceanogr. 46*:164–177.

Montgomery, M. T., T. J. Boyd, B. J. Spargo, R. B. Coffin, J. K. Steele, D. M. Ward, and D. C. Smith. 1999. Bacterial assemblage adaptation in PAH-impacted ecosystems. In: *In Situ and On-Site Bioremediation*, Vol. 5(8), ed. B. C. Alleman and A. Leeson, 223–228. Columbus, OH: Battelle Press.

Pohlman, J. W., R. B. Coffin, C. S. Mitchell, M. T. Montgomery, B. J. Spargo, J.K. Steele and T. J. Boyd. 2002. Transport, deposition, and biodegradation of particle bound polycyclic aromatic hydrocarbons in a tidal basin of an industrial watershed. *Environ. Monitor. Assess. 75*:155–167.

Polerecky, L., N. Volkenborn, and P. Stief. 2006. High temporal resolution oxygen imaging in bioirrigated sediments. *Environ. Sci. Technol. 40*:5763–5769.

Rasmussen, H., and B. B. Jorgensen. 1992. Microelectrode studies of seasonal oxygen uptake in a coastal sediment: Role of molecular diffusion. *Mar. Ecol. Prog. Ser. 81*:289–303.

Roch, F., and M. Alexander. 1997. Inability of bacteria to degrade low concentrations of toluene in water. *Environ. Toxicol. Chem. 16*:1377–1383.

Schaffner, L. C., R. M. Dickhut, S. Mitra, P. W. Lay, and C. Brouwer-Riel. 1997. Effects of physical chemistry and bioturbation by estuarine macrofauna on the transport of hydrophobic organic contaminants in the benthos. *Environ. Sci. Technol. 31*:3120–3125.

Simon, M., and F. Azam. 1989. Protein content and protein synthesis rates of planktonic marine bacteria. *Mar. Ecol. Prog. Ser. 51*:201–213.

Smith, D. C., and F. Azam. 1992. A simple, economical method for measuring bacterial protein synthesis rates in seawater using ^{3}H-leucine. *Mar. Microb. Food Webs 6*:107–114.

Tang, Y. J., S. D. Carpenter, J. W. Deming, and B. Krieger-Crockett. 2006. Depth-related influences on biodegradation rates of phenanthrene in polluted marine sediments of Puget Sound, WA. *Mar. Poll. Bull. 52*:1431–1440.

Tuominen, L. 1995. Comparison of leucine uptake methods and a thymidine incorporation method for measuring bacterial activity in sediment. *J. Microbiol. Methods 24*:125–134.

Wenzhöfer, F., and R. N. Glud. 2004. Small-scale spatial and temporal variability in benthic O_2 dynamics of coastal sediments: Effects of fauna activity. *Limnol. Oceanogr. 49*(5):1471–1481.

Zhang, X., and L. Y. Young. 1997. Carboxylation as an initial reaction in the anaerobic metabolism of naphthalene and phenanthrene by sulfidogenic consortia. *Appl. Environ. Microbiol. 63*:4759–4764.